

Efficient Incorporation of Mg in Solution Grown GaN Crystals

Jaime A. Freitas, Jr.*, Boris N. Feigelson, and Travis J. Anderson

Naval Research Laboratory, Washington, D.C. 20375, U.S.A.

Received August 13, 2013; accepted September 19, 2013; published online October 11, 2013

Detailed spectrometry and optical spectroscopy studies carried out on GaN crystals grown in solution detect and identify Mg as the dominant shallow acceptor. Selective etching of crystals with higher Mg levels than that of the donor concentration background indicates that Mg acceptors incorporate preferentially in the N-polar face. Electrical transport measurements verified an efficient incorporation and activation of the Mg acceptors. These results suggest that this growth method has the potential to produce p-type doped epitaxial layers or p-type substrates characterized by high hole concentration and low defect density. © 2013 The Japan Society of Applied Physics

II-nitride material scientists have strived in the last two decades to realize the growth of large area GaN wafers. Presently, only hydride vapor phase epitaxy (HVPE) and ammonothermal growth methods have produced commercial quality substrates.^{1–3} The first method, a fast quasi-bulk growth technique, uses sacrificial substrates to produce up to 6 in. diameter wafers, or boules of 2 in. diameter and ~0.5 in. thickness.^{4,5} The ammonothermal method, a low-growth-rate process with multi-seeded capability, produces boules of 2 in. diameter of selected crystal orientations.⁶ HVPE wafers are in general n-type (free carrier concentration of typically $\geq 5 \times 10^{17}/\text{cm}^{-3}$), have a high dislocation density (commonly $\geq 1 \times 10^7/\text{cm}^{-2}$) and poor flatness.⁷ Ammonothermal GaN wafers typically have a very high concentration of free electrons (typically $\geq 5 \times 10^{18}/\text{cm}^{-3}$), but they are very flat and have a very low dislocation density ($\sim 1 \times 10^4/\text{cm}^{-2}$).⁸ Both techniques can produce electrically isolating substrates by doping with impurities that yield deep compensating levels. However, substrates with reproducible low free electron background and p-type conductivity are still not fully realized. Therefore, the development of a method that yields GaN substrates with full simultaneous control of the electrical and crystalline properties is most desirable.

Recently, we reported that GaN crystal platelets, needles, and epitaxial films could be grown from solution at N₂ pressures of 1–3 atm and temperatures between 750 and 850 °C in a Ga–Li–GaN system.⁹ The homoepitaxial films were characterized by improved crystalline and optical properties as compared with those of commercial HVPE substrates.¹⁰ Previous studies of self-nucleated crystals indicate that these crystals have an X-ray rocking curve full width at half maximum (FWHM) similar to that of Ammonothermal crystals, record small FWHM of the first-order allowed optical phonons, and relatively low room temperature (RT) free carrier concentrations.^{11,12}

The samples used in this experiment were grown in a custom-designed reactor incorporated in a vertical tube furnace. A multi-component solvent was employed to dissolve the GaN source and subsequently grow single crystal GaN from the solution. Details of the solvent selection and preparation are described in Ref. 9. To reduce oxygen contamination, all precursor handling and crucible charging were carried out in a glove box under nitrogen atmosphere, with O₂ and H₂O contents below 1 ppm level. After crucible loading, the reactor was pumped and purged multiple times to achieve a pure nitrogen atmosphere. The crucible position in the reactor was set to induce an axial thermal gradient inside the solution. Growth runs were

conducted under purified nitrogen flow at pressures between 0.23 and 0.25 MPa and temperatures near 750–800 °C. The crucible contents were washed with deionized (DI) water and hydrochloric acid to dissolve the remaining compounds. Bulk hexagonal-shaped GaN crystalline platelets of 4 to 6 mm² area and 0.025–0.04 mm thickness were selected for characterization studies. FWHM of the X-ray diffraction rocking curve and A1(LO) phonon of single-domain platelets are similar to those reported in Ref. 10, typically ~16 arcsec and ~7.0 cm⁻¹, respectively. These values are consistent with high crystalline quality and low n-type background free carrier concentration.

A thorough study was carried out to verify the intrinsic optical and electronic properties of self-nucleated crystals grown in solution. Detailed photoluminescence (PL) and secondary ion mass spectrometry (SIMS) were performed to identify the incorporated impurities. RT and low-temperature (LT) PL measurements were employed to investigate the optical properties of the GaN crystals. For the LT measurements (~1.5–6 K), the samples were placed in a continuous-flow He cryostat with temperature variation capability between 1.5 and 300 K. Luminescence was excited with the 325 nm line of a He–Cd laser with a typical incident power between 15 and 700 μW. Neutral density filters were used to maintain the incident power within desired limits to avoid heating of the samples and to allow the observation of recombination processes with different time constants. The emitted light was dispersed by a 1800 grooves/mm 0.85 m double-grating spectrometer and detected by a UV-sensitive GaAs photomultiplier coupled to a computer-controlled photon counter system. A number of crystals characterized by relatively large spectral intensity variations of various emission bands were selected for this study, to provide insight on the optical and electronic properties of crystals grown by this method. Selective etching was employed to identify the N- and Ga-polar faces of the samples. SIMS, and low and RT PL experiments were carried on both pristine faces of the crystals to verify potential preferential impurity incorporation. Electrical characterization was performed on a probe station at RT in a front–front and front–back configuration. Current–voltage (*I*–*V*) characteristics were measured with a HP4145B semiconductor parameter analyzer, and capacitance–voltage (*C*–*V*) measurements were performed using a HP4275 LCR meter.

RT PL measurements were performed on a large number of samples from different growth batches, in an attempt to verify the correlation between spectral intensity distribution with impurities incorporation and growth conditions, and

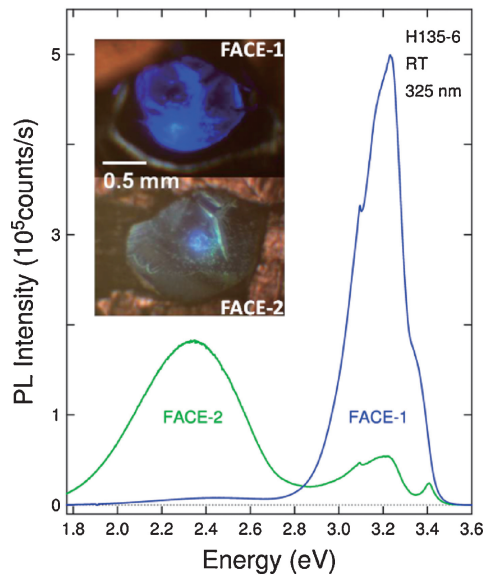


Fig. 1. Low resolution RT PL spectra of front and back faces (Face-1 and Face-2, respectively) of a platelet from the growth batch H-135. The LT spectrum of a crystal from the same growth batch is shown in Fig. 3. The figure insert depicts the RT real color luminescence imaging of both faces of the crystal (Face-1 at the top, and Face-2 at the bottom) illuminated with the 325 nm He–Cd laser line. The sample was sandwiched between copper meshes and aluminum foils to allow sequential measurement of both faces. The scale bar is 0.5 mm.

to obtain quick insights on the electronic properties of unintentionally doped (UID) crystals. Samples were selected by illumination with an unfocused 325 nm line of the He–Cd laser. During this process, it was observed that crystals from different growth batches had a dominant violet or yellow/green emission. Also, it was observed that the opposite face of samples from growth batches characterized by intense violet emission would emit mostly yellow/green light at RT. These observations suggest that, first, the growth condition affects the impurity incorporation, and second, there is a clear dependence of the impurity incorporation on the crystal surface polarity. It was found that crystals grown at a lower temperature (near 750 °C) have one face emitting an intense violet light, while both faces of crystals grown at higher temperature (near 800 °C) emit a dominant yellow/green light. Figure 1 depicts the low-resolution RT PL spectra of both faces of a crystal from the H135 growth run. The real color (RGB) PL imaging of Face-1 of this sample is highlighted in the inset and clearly shows a uniform and dominant violet emission. The spectrum of Face-1 is dominated by a recombination process with a peak at 3.25 eV, while that of Face-2 has a stronger contribution from the yellow/green defect band near 2.35 eV and smaller contributions from the 3.25 and ~3.4 eV bands. The ~3.4 eV emission results from the overlapping of contributions from recombination processes involving electrons in the conduction band and holes from the valence bands (band-to-band), since, at RT, the majority of the shallow donors transfer their electrons to the bottom of the conduction band due to thermoionization, and also from recombination processes involving free exciton with holes from the A, B, and C valence bands. The 3.25 eV band is associated with the recombination process involving electrons in the conduction

band with holes bound to the acceptor (free-to-bound or F-B). Samples with RT PL spectra of Face-1 characterized by a small contribution from the 3.25 eV emission band do not show the 3.25 eV emission band in the spectrum of Face-2, which is usually dominated by the 3.4 eV and the yellow/green bands. Despite that, the LT spectra from both faces of such samples still show a small spectral contribution due to recombination process involving shallow donor and shallow acceptor. These observations indicate that the incorporation of shallow donor and acceptor depends largely on the growth temperature and crystal face polarity. The RT spectrum of Face-1 of the sample from batch H135, highlighted in Fig. 1, shows only an intense 3.24 eV band, indicating that the recombination is dominated by the F-B process. The lack of the NBE emission and yellow-green bands suggests that the Fermi level has moved deeper into the forbidden gap toward the acceptor energy level due to a large excess of neutral acceptors.

SIMS measurements were carried out on both faces of selected samples to identify the chemical nature and concentration of the incorporated impurities. The concentration levels of O and Si were typically $\sim 5 \times 10^{16}$ and $5 \times 10^{15} - 1 \times 10^{16}$ atoms/cm³, respectively, which are close to their detection limits. The concentrations of C and H were at detection limits, but they cannot be ruled out as very low level contaminants. The Li concentration range is $(1-6) \times 10^{17}$ atoms/cm³ (detection limit $\sim 1 \times 10^{14}$ atoms/cm³), which is not surprising considering that Li₃N is one of the precursors of the growth method. Nevertheless, no additional emission band has been observed in the probed spectral region that could be attributed to Li impurity. This spectroscopic study also verified that Mg was incorporated in the samples with concentration between 3×10^{17} and 2×10^{18} atoms/cm³. In addition, it was observed that one of the sample faces always had at least one order of magnitude lower Mg doping level. Gas discharge mass spectrometry (GDMS) of the Li₃N precursor detected a background concentration of 6.6 ppm Mg indicating that this was source of Mg doping. A comparison between SIMS and GDMS results consistently indicates an efficient incorporation of Mg in the GaN crystal.

Chemical etching provides a simple approach to distinguish between the Ga and N polar faces of GaN, due to their different etch rates in KOH.¹³⁾ Selective chemical etching was performed on two crystals platelets characterized by bright RT violet emission. Two crystals from the H135 batch were mounted on a platinum foil with either the violet or yellow/green emitting face up, and etched in 2M KOH at 100 °C for a few minutes. It was observed that only the crystal whose face emits the violet light under UV excitation at RT was attacked by the etching solution (which is indicative of the N-polar surface), as depicted in Figs. 2(a) and 2(b). This result clearly indicates that the N-polar surface incorporates larger amount of Mg than the Ga-polar face. One possible explanation of this observation may be related to the lifetime of Mg adatoms on the N-polar face during the growth, which is expected to be larger than on the Ga-polar face due to the GaN atomic structure. A lower growth temperature may increase the Mg adsorption lifetime during the growth, resulting in higher Mg incorporation, as was observed for GaN crystals grown at temperatures near 750 °C.

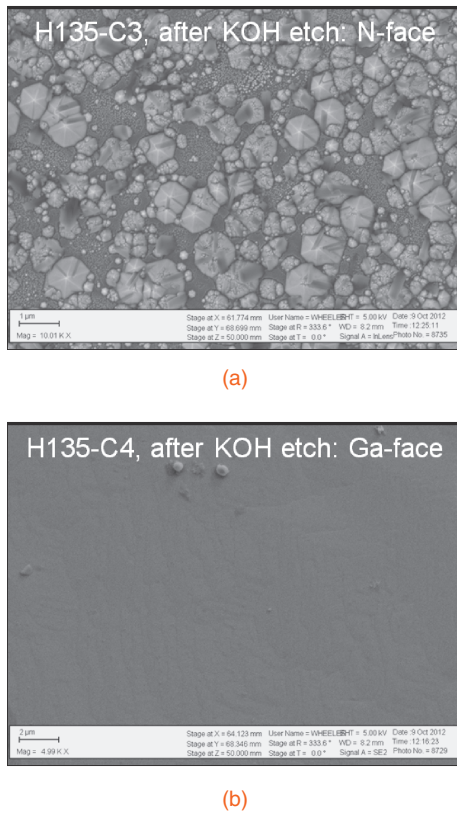


Fig. 2. Scanning electron microscopy image of the sample H135-3 after minutes of 2 M KOH etch. The formation of etch pits is consistent with the N-face polarity (a). These pits are not observed on the opposite face of similar sample submitted simultaneously to the same chemical etching procedure (b).

LT PL experiments were carried out on both faces of a sample from growth run C80, grown under similar conditions to the samples from the H135 batch, to identify the nature of the recombination processes detected in the measured spectral range. Figure 3 shows the LT PL spectra of the N- and Ga-polar faces of a crystal, from the growth batch C80, acquired in the spectral range between 1.77 and 3.78 eV. The spectra are dominated by an intense peak near 3.47 eV associated with the annihilation of free excitons and excitons bound to shallow donor and acceptor impurities, commonly called “near-band-edge” (NBE) emission band. These recombination processes have one phonon replica (1LO-NBE) around 3.38 eV. The intense broad band resulting from multiple overlapping peaks is assigned to the recombination process involving the annihilation of electrons localized at neutral shallow donors (Si and/or oxygen) with holes localized at Mg neutral shallow acceptors, represented by “DAP & Phonon Replicas” in Fig. 3. The first peak observed at ~ 3.27 eV is non phonon or zero-phonon line (ZPL) DAP recombination band and does not involve phonons in the recombination process. The additional peaks are DAP phonon replicas which are displaced toward the low-energy side of the ZPL-DAP band by multiples of 92 meV, the energy of the strongly coupling A1(LO) phonon. These spectra also show a weak yellow band (at ~ 2.25 eV, ~ 551 nm) and/or the green band (at ~ 3.27 eV, ~ 523 nm).

The high-resolution PL spectrum of the same samples measured at 6 K in the spectral region assigned to the NBE

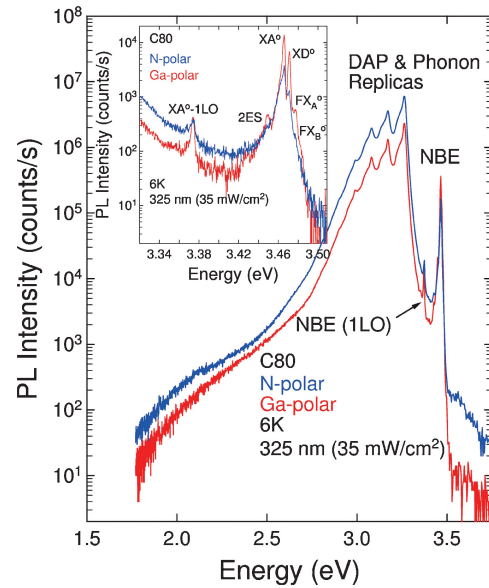


Fig. 3. LT and low resolution PL spectra of the Ga- and N-polar faces of a self-nucleated GaN crystal. Changes in the relative intensity of the DAP and NBE emission bands (see text) results from the variation in the concentration of donors and acceptors. The figure insert show the LT PL spectra of the same sample acquired at higher resolution conditions. The changes in the relative intensity of the near band edge emission components ($X_A D^\circ$, $X_A A^\circ$, FX_A° , and FX_B°) results from the variation in the concentration of neutral donors and acceptors.

emission (between 3.51 and 3.32 eV) is depicted in the inset of Fig. 3. The spectrum of the Ga-polar face include emission lines associated with recombination processes involving the annihilation of free excitons with holes deriving from valence band A (FX_A) and valence band B (FX_B). The intense line assigned to the annihilation of excitons bound to neutral shallow donors (Si and/or O), which leave the donors in the ground states ($X_A D^\circ$), is observed at 3.471 eV.¹⁴ The line related to the annihilation of exciton bound to a neutral Mg shallow acceptor ($X_A A^\circ$) is observed at 3.465 eV. In contrast, only a very weak $X_A D^\circ$ emission line is observed in the high-resolution spectra of the N-polar face. This observation is consistent with efficient compensation of the shallow donors by increased incorporation of the neutral Mg shallow acceptor.¹⁵ Additionally, the emission line associated with the recombination process leaving the donors in the excited states (two electron satellite or 2ES) at 3.449 eV, weakly observed in the spectrum of Ga-polar face, is not present in the PL spectrum of N-polar face. This observation is also consistent with a relatively higher concentration of background shallow acceptor impurities in N-polar face.¹⁵ Furthermore, the sharp $X_A A^\circ$ line shape in the Ga-polar face spectrum is considerably broader in the N-polar face spectrum, indicating higher Mg acceptor concentration in the N-polar face.¹⁶ The evidence of increasing incorporation of Mg acceptors in the N-polar face is corroborated by increased relative intensity of the DAP band. No evidence of a second acceptor or spectral intensity variation was observed in any sample, even after hours of high-intensity light soaking.¹⁷ The very low level of H in these crystals and the stability of their excitonic spectra strongly indicate that the shallow Mg acceptor is a substitutional isolated impurity for Ga, and is not complexing

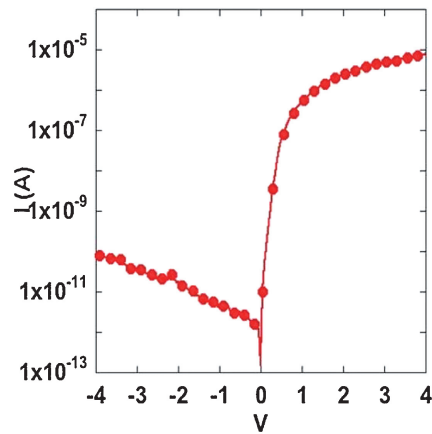


Fig. 4. I - V curve of one of the H-135 batch sample, showing the typical curve of a p-n junction with small leakage current.

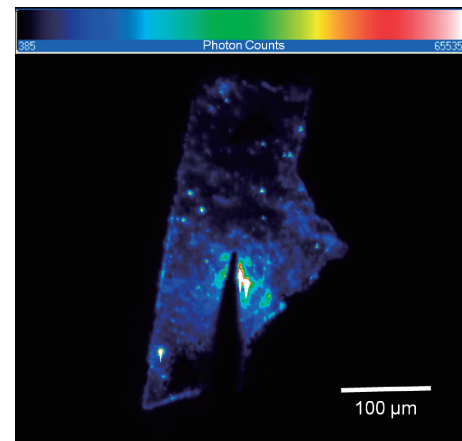


Fig. 5. False color electroluminescence image of a small sample from the H135-B.

with any impurity or structural defect.¹⁸⁾ It was also observed during the excitation intensity experiments that these crystals have excitonic related peak intensities 500 to 1000 times larger than that observed from MBE-deposited homoepitaxial films with the same level of Mg doping.¹⁹⁾ Considering that the yellow/green band associated with deep gap levels is observed in both kinds of sample, it is fair to assume that the bulk GaN crystals grown from solution have a considerably lower concentration of non radiative defects or defects that emit outside of the measured spectral range.

C - V measurements carried out on the bright violet-emitting face of one sample indicated p-type conductivity with a RT hole concentration of 5×10^{16} holes/cm³. This value is consistent with the efficient incorporation and activation of unintentional Mg impurity, and relatively low compensation of the GaN crystals. The C - V measurement performed on the opposite face of the crystal indicated n-type conductivity. The differences in electrical properties of the N- and Ga-polar faces of these samples justify I - V measurements in a vertical configuration across these samples. The I - V curve of sample #3 of batch H-135, as highlighted in Fig. 4, shows rectifying characteristics. The result indicates that a p-n junction with low reverse leakage is formed in the bulk of the sample, confirming the strong preferential incorporation of different type of impurities on opposite GaN polarity. Figure 5 depicts a false color electroluminescence image of a similar sample from the same growth run, demonstrating that a p-n junction is naturally formed by the solution growth method.

In summary, thorough spectrometric and optical spectroscopic studies in combination with selective etching carried out on samples grown by the moderate-pressure solution method demonstrate that shallow substitutional Mg impurities efficiently and preferentially incorporate on the N-polar face of the GaN crystals, and that lower growth temperatures favor larger Mg incorporation. The relatively higher PL efficiency consistently indicates that these crystals have a much lower concentration of non radiative defects than Mg doped MBE homoepitaxial films deposited on HVPE substrates.

I - V and electroluminescence studies verified that a p-n junction characterized by a small leakage current is formed in the bulk of the samples. These results strongly suggest that liquid phase epitaxial growth of GaN films on N-polar face substrates may be a viable approach to achieve layers with higher hole concentrations.

- 1) T. Yoshida, Y. Oshima, T. Eri, K. Ikeda, S. Yamamoto, K. Watanabe, M. Shibata, and T. Mishima: *J. Cryst. Growth* **310** (2008) 5.
- 2) D. Hanser, M. Tutor, E. Preble, M. Williams, X. Xu, D. Tsvetkov, and L. Liu: *J. Cryst. Growth* **305** (2007) 372.
- 3) R. Dwilinski, R. Doradzinski, J. Garczynski, L. P. Sierzputowski, A. Puchalski, Y. Kanbara, K. Yagi, H. Minakuchi, and H. Hayashi: *J. Cryst. Growth* **300** (2007) 11.
- 4) K. Motoki, T. Okahisa, R. Hirota, S. Nakahata, K. Uematsu, and N. Matsumoto: *J. Cryst. Growth* **305** (2007) 377.
- 5) D. Hanser, L. Liu, E. A. Preble, K. Udwaray, T. Paskova, and K. R. Evans: *J. Cryst. Growth* **310** (2008) 3953.
- 6) R. Kucharski, M. Rudziński, M. Zajac, R. Doradzinski, J. Garczynski, L. P. Sierzputowski, R. Kudrawiec, J. Serafińczuk, W. Strupiński, and R. Dwilinski: *Appl. Phys. Lett.* **95** (2009) 131119.
- 7) R. P. Vaudo, X. Xu, C. Loria, A. D. Salant, J. S. Flynn, and G. R. Brandes: *Phys. Status Solidi A* **194** (2002) 494.
- 8) N. A. Mahadik et al.: in preparation.
- 9) B. N. Feigelson, J. K. Hite, N. Y. Garces, J. A. Freitas, Jr., J. G. Tischler, and P. B. Klein: *J. Cryst. Growth* **312** (2010) 2551.
- 10) B. N. Feigelson, R. M. Frazier, M. Gowda, J. A. Freitas, Jr., M. Fatemi, M. A. Mastro, and J. G. Tischler: *J. Cryst. Growth* **310** (2008) 3934.
- 11) N. Y. Garces, B. N. Feigelson, J. A. Freitas, Jr., J. Kim, R. Myers-Ward, and E. R. Glaser: *J. Cryst. Growth* **312** (2010) 2558.
- 12) J. A. Freitas, Jr., J. G. Tischler, N. Y. Garces, and B. N. Feigelson: *J. Cryst. Growth* **312** (2010) 2564.
- 13) C. Lee, J. K. Hite, M. A. Mastro, J. A. Freitas, Jr., C. R. Eddy, Jr., H.-Y. Kim, and J. Kim: *J. Vac. Sci. Technol. A* **30** (2012) 040602.
- 14) J. A. Freitas, Jr., W. J. Moore, B. V. Shanabrook, G. C. B. Braga, S. K. Lee, S. S. Park, and J. Y. Han: *Phys. Rev. B* **66** (2002) 233311.
- 15) E. Molva and N. Magna: *Phys. Status Solidi B* **102** (1980) 475.
- 16) J. Lee, E. S. Koteles, M. O. Vassell, and J. P. Salerno: *J. Lumin.* **34** (1985) 63.
- 17) B. Monemar, P. P. Paskov, G. Pozina, C. Hemmingsson, J. P. Bergman, T. Kawashima, H. Amano, I. Akasaki, T. Paskova, S. Figge, D. Hommel, and A. Usui: *Phys. Rev. Lett.* **102** (2009) 235501.
- 18) B. Monemar, S. Khromov, G. Pozina, P. Paskov, P. Bergman, C. Hemmingsson, L. Hultman, H. Amano, V. Avrutin, X. Li, and H. Morkoç: *Jpn. J. Appl. Phys.* **52** (2013) 08JJ03.
- 19) E. R. Glaser, M. Murthy, J. A. Freitas, Jr., D. F. Storm, L. Zhou, and D. J. Smith: *Physica B* **401–402** (2007) 327.